Hysteresis and fractional matching in thin Nb films with rectangular arrays of nanoscaled magnetic dots

O. M. Stoll and M. I. Montero
University of California San Diego, Physics Department 0319, 9500 Gilman Drive, La Jolla, California 92093

J. Guimpel
Centro Atómico Bariloche & Instituto Balseiro, Comisión Nacional de Energía Atómica & Universidad Nacional de Cuyo, San Carlos de Bariloche, 8400 Río Negro, Argentina

Johan J. Åkerman* and Ivan K. Schuller
University of California San Diego, Physics Department 0319, 9500 Gilman Drive, La Jolla, California 92093
(Received 26 July 2001; revised manuscript received 16 October 2001; published 28 February 2002)

We have investigated the periodic pinning of magnetic flux quanta in thin Nb films with rectangular arrays of magnetic dots. In this type of pinning geometry, a change in the periodicity and shape of the minima in the magnetoresistance occurs for magnetic fields exceeding a certain threshold value. This was explained recently in terms of a reconfiguration transition of the vortex lattice due to an increasing vortex-vortex interaction with increasing magnetic field. In this picture the dominating elastic energy at high fields forces the vortex lattice to form a square symmetry, rather than being commensurate with the rectangular geometry of the pinning array. In this paper we present a comparative study of rectangular arrays with Ni dots, Co dots, and holes. In the magnetic dot arrays we found a strong fractional matching effect up to the second-order matching field. In contrast, no clear fractional matching is seen after the reconfiguration. Additionally, we discover the existence of hysteresis in the magnetoresistance in the crossover between the low- and high-field regimes. We find evidence that this effect is correlated with the reconfiguration phenomenon rather than to the magnetic state of the dots. The temperature and angular dependences of the effect are measured, and possible models are discussed to explain this behavior.

DOI: 10.1103/PhysRevB.65.104518 PACS number(s): 74.60.Ge, 74.60.Jg, 74.76.Db

I. INTRODUCTION

The study of vortex pinning and dynamics in type-II superconductors is essential for all prospective applications in which high current densities or magnetic fields are involved. The rich diversity of different phases found in the mixed state of high-temperature superconductors[1,2] shows that vortex pinning and dynamics are also highly interesting from a fundamental point of view.

Nanolithography provides a method to produce ordered arrays of artificial pinning centers on the scale of the superconducting coherence length ξ and the magnetic penetration depth λ. With these nanoscaled pinning centers it is possible to ''engineer'' the pinning force of a type-II superconductor such that the critical current j_c is increased for specific magnetic fields (matching fields). Such arrays can consist of holes (antidots),[3–6] magnetic dots,[7,8] or magnetic particles accumulated in a Bitter decoration experiment.[9] An interesting application for periodic antidot arrays is the reduction of $1/f$-flux noise in superconducting quantum interference devices.[10] Arrays of nanoscaled dots were prepared with various magnetic[11,12] and nonmagnetic materials[13] and with different array geometries such as triangular,[7] square,[8] Kagome,[14] and rectangular.[15]

Rectangular arrays seem to be particularly interesting, since a distinct change in the flux-pinning characteristics was observed above a certain magnetic threshold field B_{tr}.[15] At this field value, the shape of the minima in the magnetoresistance as well as their periodicity changes. This behavior has been explained by means of a geometrical reconfiguration transition of the vortex lattice. In this model, two competing energies are considered to be important: At a low magnetic field B, the pinning energy E_{pin} dominates over the elastic energy E_{el} of the vortex lattice, and the vortices are dragged onto the artificial pinning centers, this way adjusting to the underlying rectangular geometry; with increasing field, E_{el} becomes more important, and at the threshold B_{tr} it forces the vortex lattice back to the intrinsic geometry, which is assumed to be square.

The pinning mechanism of the vortices by the magnetic dots is still not completely understood. It is believed that a large component of the pinning force is of magnetic origin.[13] Another contribution is likely to come from the geometrical modulation of the superconducting Nb film due to the underlying dots.[11] Whether the periodic pinning is mainly caused by a magnetic interaction with the stray fields of the dots, by the proximity effect, or by a combination of different mechanisms still remains unresolved. Intentional manipulations of the magnetic domain structure of the dots show that a magnetic influence does exist in the sense that the pinning force increases with stronger stray fields.[12]

Another important issue arises if we consider the fact that a strong matching effect can be observed in electric transport measurements with magnetic dots. Since vortices need to move in order to produce electric dissipation, not only the static matching but also the dynamics of the flux quanta will play an important role for the signal. Particularly in the high-field part of the magnetoresistance, the critical current j_c will

TABLE I. Sample characteristics. d_{dot} is the dot diameter, t_{Nb} and t_{dot} are the Nb film thickness and the dot thickness, respectively. In the case of the holes t_{dot} is the hole depth.

	Dot material	T_c	ΔT_c	d_{dot}	t_{Nb}	t_{dot}
Sample 1	Ni	8.2 K	0.093 K	300 nm	75 nm	38 nm
Sample 2	Co	8.3 K	0.115 K	300 nm	75 nm	30 nm
Sample 3	holes	6.94 K	0.12 K	300 nm	80 nm	120 nm

be low compared to the applied transport current j, so that dynamical effects can be expected. It is known that a moving vortex lattice can undergo dynamical phase transitions[16] and order itself at higher flux velocities.[17–19] The systems described in those references contain a random distribution of defects, but the same effect can also be seen with artificial periodic arrays of pinning centers.[20]

It appears that a study focused on the high-field regime of the rectangular pinning arrays, where the reconfiguration transition occurs, has the potential of providing insight into the dynamical nature of the matching effect and the pinning mechanism in general. Therefore, in this paper we present experiments done exclusively on samples with rectangular arrays of magnetic dots. We focus specifically on the behavior of these samples before and after the reconfiguration. We find evidence of a fractional matching effect before the change of regime as well as hysteresis effects occurring in the reconfiguration region. We discuss these effects in the framework of two possible models: a geometrical reconfiguration model, and a model allowing the dots to accommodate multiple vortices.

II. EXPERIMENT

The pinning arrays were prepared by means of *e*-beam lithography. A detailed description of the sample preparation can be found in Refs. 7 and 21 for the magnetic dots and Ref. 22 for the holes. In brief, PMMA is spun on top of a (100) Si substrate. After the *e*-beam writing process, the material for the dots is deposited using dc-magnetron sputtering (Ni) and *e*-beam evaporation (Co), respectively. Alternatively, holes can be etched into the substrate using reactive ion etching. A lift-off process removes the PMMA including the unwanted material. The remaining dots have a typical thickness of 30 nm and a typical diameter of 300 nm. In both cases, a superconducting Nb film with a thickness of about 100 nm is sputtered on top of the array. For a similar Nb film which was prepared using the same process parameters, we determined a surface roughness of ± 7 Å and a top oxide thickness of 34 Å from low-angle x-ray-diffraction data.

The results we present in this paper were obtained for three different samples. For all of these samples we used rectangular $(a \times b)$ pinning arrays with an aspect ratio $r = b/a = 900\ \text{nm}/400\ \text{nm} = 2.25$. The arrays of samples 1 and 2 were made of Ni and Co dots, respectively, while for sample 3 the pinning array consisted of 120-nm-deep holes in the Si substrate. A statistical analysis of 20 dots in a scanning electron micrograph for sample 2 indicates a circular shape of the dots, i.e., the horizontal and vertical diameters coincide within a standard deviation of 5%. An estimate of the absolute difference between the mean horizontal and vertical diameters yields 8 ± 6 nm. The T_c of the samples was in a range between 6.94 and 8.2 K, with a superconducting transition width of the order of 0.1 K for all three films. The relevant parameters for the three samples are summarized in Table I. The magnetoresistance was measured in a standard four-probe microbridge geometry with a bridge width $w = 40\ \mu$m and a length $L = 50\ \mu$m between the voltage leads.

The measurements were performed in a helium cryostat with a 80 kG superconducting magnet, with the magnetic field oriented perpendicular to the film surface. In some of the measurements a rotatable sample holder was used to vary the angle θ between the film normal and the magnetic field. The transport current was always kept perpendicular to the field direction. It was applied along the long side b of the rectangular array. Thus the Lorentz force always drove the vortices along the short side a.

The voltage drop over the measurement bridge is measured with a lock-in amplifier which also serves as a supply for the transport current. The current density is typically in a range from 0.3 to 3 kA/cm^2. The electric current for the magnetic field was provided by a Kepco model BOP20-20 M current source, and measured as a voltage drop on a resistor mounted in a series with the magnet leads. With our current experimental setup we can reach magnetic-field resolutions as high as 0.1 G over a total range from -2 to 2 kG. The sweep rate was typically between 0.2 and 2 G/s. The measurements were found to be independent of the sweep rate within this range. In order to test for possible effects due to the ac-transport current, the frequency of the lock-in amplifier was varied between 17 Hz and 20 kHz, yielding identical results for the magnetoresistance.

III. EXPERIMENTAL RESULTS

A. Fractional matching

Figure 1 shows the positive part of a typical magnetoresistance curve measured with sample 1. It was recorded using a magnetic field resolution of 0.1 G, which is about a factor of 50 better than in our previous experiments. In the experiment shown, the magnetic field was increased from 0 to 600 G with a rate of about 0.2 G/s. Clearly two different regimes can be identified in the curve. At low fields there are sharp and well-defined minima similar to the ones seen in previous measurements with square[8,7] and rectangular arrays of magnetic dots.[15] The positions can be accurately described by the nth-order matching fields $B_n = n(\phi_0/a \cdot b)$, where $\phi_0 = 20.7\ \text{G}\,\mu\text{m}^2$ is the magnetic flux quantum and n is an

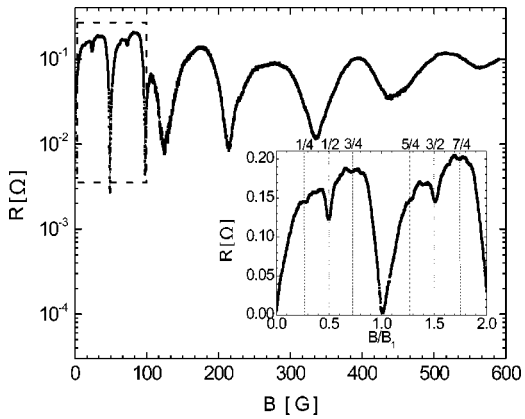

FIG. 1. Magnetoresistance of sample 1 (Ni dots) measured at $T=7.8$ K with $I=0.2$ mA. Only the positive part of the curve is shown. The dashed rectangle marks the low-field part. The inset shows a magnification of the part of the curve marked with the dashed rectangle. The magnetic field is normalized with the first-order matching field B_1. Field values corresponding to fractional matching are highlighted with dashed lines.

integer number. Thus, from the experimental values for sample 1 in Fig. 1, we can determine $a\times b=0.421\ \mu\mathrm{m}^2$, with an error of 0.6% resulting from the resolution limit of the electronic setup.

Apart from the well-known integer matching fields, there are additional structures visible in the low-field part of the curve which is marked with a dashed rectangle. These can be easily identified as the half-integer matching fields for $n=\frac{1}{2}$ and $\frac{3}{2}$. To the best of our knowledge fractional matching has not yet been observed in rectangular arrays of magnetic dots. The inset of Fig. 1 shows an enlargement of the marked part of the curve. Here, even finer structures can be observed. The values corresponding to multiples of the $\frac{1}{4}$ and $\frac{1}{2}$ fractions of the integer matching fields are highlighted with dashed lines. They clearly coincide with the respective dips in the magnetoresistance. The minima for ''quarters'' are much shallower than the ones for ''halves,'' in agreement with the fractional matching seen in hole arrays.[23] We emphasize that fractional matching can be clearly seen up to the second-order matching field. The depth of the minima, and therefore the corresponding pinning strength, is comparable for the fractional minima $n=1/2$ and 3/2 (see Fig. 1). In Fig. 2, we note that the fractional matching effect at half-integer fields is also clearly visible in sample 2, which demonstrates the reproducibility of this effect independent of the dot material.

At magnetic fields higher than the threshold value B_{tr}, the behavior changes drastically, as described by the previously mentioned reconfiguration transition of the vortex lattice.[15] In this regime, the series of matching peaks seems to be well described by $B_n=n(\phi_0/a^2)$, a being the short side of the rectangle, along which the Lorentz force is applied. The vortex lattice literally ''loses memory'' of the larger lattice period b. Regarding the fractional matching in this regime, we see that, within our experimental resolution, there is no observable fine structure. It appears that the fractional matching

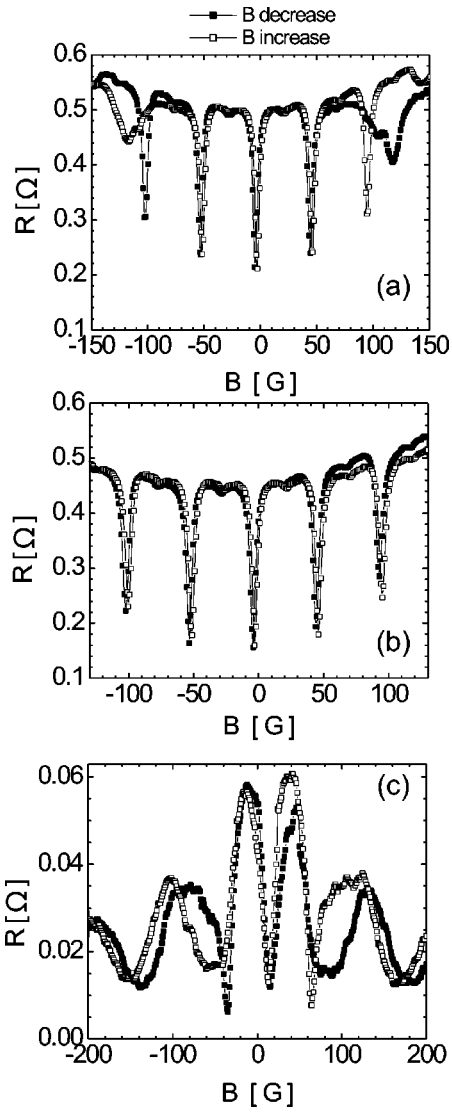

FIG. 2. Hysteretic effect of the magnetoresistance. Curves with open and filled squares correspond to a increase and a decrease of the magnetic field, respectively. (a) Magnetoresistance of sample 2 (Co dots) measured at $T=7.8$ K with $I=0.2$ mA. In this experiment the field initially exceeded the values $\pm B_{\mathrm{tr}}$ for the respective curves before the recording was started. (b) Magnetoresistance for the same sample at $T=7.8$ K and $I=0.2$ mA. Here the field was kept below $\pm B_{\mathrm{tr}}$. (c) Magnetoresistance of sample 3, consisting of an array of holes measured at $T=6.5$ K with $I=0.2$ mA.

is absent or at least much weaker than for fields $B<B_{\mathrm{tr}}$. We discuss possible implications of this result in Sec. IV of this paper.

B. Hysteretic effect

We found another interesting effect in our samples with rectangular arrays of magnetic dots. When the magnetic field is first increased (or decreased) to a high positive (or negative) start value and then subsequently swept to zero and further to negative (or positive) fields, a distinct asymmetry appears in the magnetoresistance. The result of such an experiment can be seen in Fig. 2(a). For the moment, we con-

centrate on the increasing field curve (open squares). Here the recording of the curve was started at an initial field $B=-150$ G. We observe a clear asymmetry in the data. It seems that the sharp low-field minimum of the order $n=-2$, which can be expected at around $B=-100$ G due to symmetry reasons, is missing. On the other hand, the minimum of the order $n=+2$ at the matching field $B=+100$ G on the positive side is clearly visible. Instead of the minimum $n=-2$, a much broader peak appears at $B\approx-120$ G which apparently matches neither the low-field periodicity if indexed as $n=-2$ nor the high-field periodicity $\Delta B=\phi_0/a^2$. It appears that under certain conditions, an ''intermediate state'' evolves for magnetic fields close to B_{tr}. If the field is subsequently swept back from 150 to -150 G [filled squares in Fig. 2(a)] the minimum of the order $n=+2$ is missing on the positive side, while the one for $n=-2$ on the negative side is visible. Apparently, the shape of the magnetoresistance curves depends strongly on the magnetic history of the sample. It is important to point out that, in the experiment in Fig. 2(a), the field has been increased above the threshold value B_{tr} and decreased below $-B_{tr}$, respectively. The fact that the observed hysteresis appears at magnetic fields close to the threshold values $\pm B_{tr}$ suggests that it may have to do with the reconfiguration transition.

In order to confirm this conjecture, we repeated the experiment keeping the magnetic field in the range between the threshold values $B_{tr}\approx\pm 140$ G, obtaining the results shown in Fig. 2(b). In this case, contrary to the data in Fig. 2(a), we obtain a fully reversible magnetoresistance curve except for a small deviation on the positive side which is probably due to a small temperature drift during the measurement. This proves that the hysteresis is related to the reconfiguration phenomenon.

Hysteretic effects in conjunction with periodic pinning phenomena were also reported in the literature. Therefore, possible implications of our results have to be discussed. A potential microscopic origin of these effects is the hysteresis due to the alignment of the magnetic moment of the dots, when the external magnetic field is swept beyond the coercive field for the perpendicular direction. An asymmetry of the critical current for samples with arrays of magnetic dots due to this mechanism was reported in Ref. 14. However, in those experiments the dots were much thicker (110 nm), and had a smaller diameter (120 nm). Thus the shape anisotropy can be expected to be much smaller than for the geometry in our experiments ($d_{dot}=300$ nm, $t_{dot}=30-40$ nm; see Table I). Still, the magnetic field used in Ref. 14 to magnetize the dots perpendicular to the film surface was around 3.5 kG, whereas in our experiment [Figs. 2(a) and 2(b)], it was always kept below 150 G. Because of the larger shape anisotropy, we can expect our dots to have their entire magnetic moment in-plane (parallel to the film surface). Also, a pronounced asymmetry effect in the magnetization of Pb films with square arrays of Pt/Co/Pt dots, which have their magnetic moment perpendicular to the plane, was observed.[12] In this work no asymmetry in the magnetization vs B characteristics was visible for dots with an in-plane magnetic moment. However, there was a small difference in the behavior before and after an initial magnetization procedure. This has been shown to be due to the formation of single domain configurations out of the as-grown multidomain arrangement. An atomic force microscopy imaging of domain walls on magnetic dots similar to the ones in our samples makes the existence of such domains likely.[24] Since the hysteresis in our case is reproducible from measurement to measurement, and since we did not find any difference between the initial sweep and the consecutive experiments, we conclude that a domain switching process either does not occur or has no visible influence on our results.

To completely exclude an effect due to a change in the effective magnetic moment of the dots, we repeated the above described experiment with a sample consisting of an array of holes in the substrate (sample 3). If the effect is due to the magnetization of the dots, this sample should obviously not show the hysteretic magnetoresistance. From the plot in Fig. 2(c) it becomes clear that hysteresis is also present and, consequently, that the magnetic moment of the dots does not play a role in its origin. The field sweeps (open squares from -200 to 200 G and filled squares from 200 to -200 G) show hysteresis like the ones with the magnetic dot arrays (samples 1 and 2). Here, probably due to the less effective pinning of the holes compared to the magnetic dots, a reconfiguration transition occurs already after the first order matching field ($n=1$). This behavior was already described in detail elsewhere.[11] Note that the lower T_c of this sample could also contribute to a weaker periodic pinning.

The results obtained so far suggest that the hysteretic effect is correlated to the reconfiguration transition appearing in rectangular arrays of magnetic dots. The fact that the magnetoresistance and the critical current for square arrays, where no reconfiguration is expected, were found to be symmetric, without showing hysteresis within the available experimental resolution[7,13] is in agreement with this result.

C. Angular and temperature dependence

The dependence of the periodic pinning on the angle θ between film normal and the magnetic field was studied for square arrays of magnetic dots.[7] It was found that only the component of the field perpendicular to the film surface $B_\perp$ matters for a vortex system,[7] i.e., that the applied magnetic field B is effectively reduced by a factor $\cos\theta$. However, this has not yet been confirmed for rectangular arrays of magnetic dots. In this geometrical configuration it is especially interesting to study whether the reconfiguration transition and/or the high-field behavior also depend only on the normal component of the field. The geometry of our experiment on rectangular arrays is sketched in Fig. 3 (lower inset). The magnetic field was tilted along the short side a of the rectangle. Therefore the Lorentz force, resulting from the current applied along the long side b, always remains parallel to the short side a. Figure 3 shows a series of magnetoresistance curves of sample 2 for values of θ between 3° and 72° as a function of the perpendicular component of the applied field $B_\perp=B\cos\theta$. We again note a pronounced asymmetry in the curve, as described earlier in this section. Furthermore the positions of the peaks scale nicely with the $1/\cos\theta$ up to

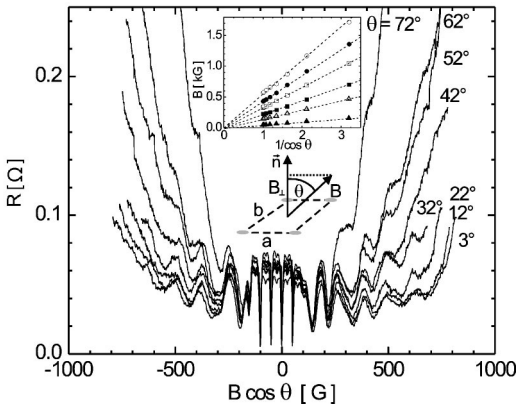

FIG. 3. Angular dependence of the magnetoresistance for sample 2. The *x* axis is normalized with the projection of the field on the normal to the film surface $B\cos\theta$. The upper inset shows a plot of the position B of the minima vs $1/\cos\theta$ for the order $n=1$ (filled triangles) through $n=6$ (open circles). The lower inset shows a sketch of the geometry used for the angular-dependent experiments. Here **n** is the normal to the sample surface, and *a* and *b* are the short and long sides of the rectangle. $B_\perp$ corresponds to the component of the magnetic field perpendicular to the surface, and B is the total applied field.

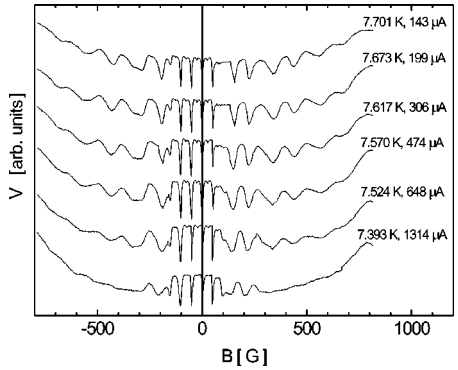

FIG. 4. Temperature dependence of the magnetoresistance for sample 2. For each curve the current was adjusted to give the same voltage of 10 μV at a field of 800 G. For clarity, the curves are shifted with respect to each other along the voltage axis.

high orders (see the upper inset of Fig. 3). This behavior is identical to that of square arrays of magnetic dots. Moreover, the position of the threshold field $\pm B_{tr}$ does not depend on the angle θ. This means that both the reconfiguration transition and the behavior of the vortex system after the reconfiguration depend only on $B_\perp$. Apparently, for the peak position only the number of vortices per unit cell of the periodic array is important, similar to what was already found for the square geometry. Nevertheless, there is a notable difference in the *absolute* value of the magnetoresistance if we compare the parts of the curve above and below $|B_{tr}|$. The low-field part $|B|<B_{tr}$ is very stable and reproducible when scaled with $B\cos\theta$. In contrast, in the high-field section the resistance increases considerably with increasing θ. It is striking that the stability of the low-field regime stretches out to about the same field values on the positive and negative side of the *x* axis, regardless of the fact that there is a minimum missing on the positive side. Up to now, we do not have a conclusive explanation for this behavior, although it could be the beginning of a transition to the normal state due to the fact that the total applied field B comes close to the B_{c2} value of our film. This explanation is slightly contradictory with the fact that the properties scale as the normal component of the field. It could indicate that the film thickness is lower but not negligible when compared to λ.

The temperature dependence of the asymmetry and of the sudden change in the periodicity of the magnetoresistance minima for the rectangular arrays can give important clues about the mechanisms involved in causing these effects. Therefore, we recorded a series of curves at different temperatures T close to T_c, which are shown in Fig. 4. For clarity, the curves are shifted with respect to each other along the voltage axis. The position of zero magnetic field $B=0$ is marked by a solid line. Because of the change of the critical current j_c with temperature, the transport current for each measurement has been adjusted such that the dissipation level at a given magnetic field remained the same for all curves. For the experiment shown in Fig. 4 we used a voltage criterion of 10 μV at a field of 800 G. For all curves, the magnetic field has first been increased to a positive start value and subsequently swept to negative values. Once again, we can see the typical asymmetry described in Sec. III B. For all of the curves, the minimum for the positive second-order matching field $n=+2$ is missing. We also observe a different temperature dependence of the positive and negative sections of the curves. On the positive side, the minimum with $n=+2$, which is suppressed for $T=7.701$ K, starts to develop with decreasing temperature, until it is clearly visible for the lowest temperature $T=7.393$ K. Because of the asymmetry the change on the negative side affects the minimum with $n=-3$. Here the minimum seems to become more pronounced (deeper) with decreasing temperature as well. However, the change is less dramatic than for $n=+2$. If we take a look at the overall shape of the curve, the low-field part $|B|<B_{tr}$ varies little with temperature on both sides. In contrast, the part after the reconfiguration $|B|>B_{tr}$ seems to be strongly T dependent. The minima are effectively ''washed out'' with decreasing T. This indicates that random pinning gains importance compared to the artificial periodic pinning as the temperature is further lowered below T_c. Apparently the random defects are much more important for the behavior after the reconfiguration transition than before it. This is a strong indication that different mechanisms are responsible for the matching phenomenon in these two parts of the curve.

IV. MODEL DISCUSSION

In the discussion of our results we will again distinguish between the two qualitatively different parts visible in our data. In the low-field regime, we have a well-defined series of resistance minima with a periodicity related to the dot unit cell area. This part will be discussed in Sec. IV A.

The high-field minima are less well defined, and their periodicity appears to be exclusively related to the side of the

dot unit cell along which the Lorentz force is applied. The transition between the two phases shows a characteristic hysteretic behavior. The high-field part and the transition between the two regimes, will be discussed in Sec. IV B.

A. Low-field phase

The low-field data are usually described in terms of two possible models. The first one, which we label the ''matched lattice'' model,[21] assumes that only one vortex can be pinned to a magnetic dot. The vortex lattice matches the dot array, and the excess vortices are forced into interstitial symmetry positions of the underlying array. Here the magnetoresistance minima are directly equivalent to maxima in the critical current. These are due to the fact that at integer numbers of vortices per unit cell of the dot lattice, there are no free interstitial positions for the vortices to jump to. In the second model, which we label as the ''multivortex model,[4]'' each magnetic dot is able to accommodate more than one vortex. This can occur either in the form of multiple confined vortices or as a single multiquanta vortex. In this model the maxima in the critical current are understood in similar terms. Now the vortices jump between the magnetic dots, and an increase in the critical current occurs whenever the number of vortices is the same on each dot, i.e., again at integer numbers of vortices per unit cell of the dot lattice. Pinning of multiple vortices to a single pinning center is possible, if the saturation number n_s is larger than 1. For an isolated hole in the superconductor, it can be estimated using the expression $n_s \approx \kappa r/2\lambda$.[25] Here κ is the Ginzburg-Landau parameter, and r is the radius of the pinning center. In a periodic array, however, n_s can be expected to be higher because the interaction with the next-neighbor vortices in the lattice is not negligible. Therefore, the saturation number will also depend on the geometry of the pinning array.

For both models, the origin of the fractional matching peaks has an explanation similar to the one sketched above for the integer-order-matching peaks. A symmetrical periodic vortex structure is formed and, in order to move the vortices, this symmetrical structure has to be broken. However, the periodicity of this fractional order structure is larger than one dot lattice unit cell, and thus the critical current enhancement (or resistivity reduction, respectively) is smaller.

The experimental data obtained at low fields seem to favor the multivortex model. A schematic illustration of the two models is shown in Fig. 5. For the matched-lattice model one expects the vortices to be pinned more strongly for magnetic fields below the first-order minimum than above it. This is due to the fact that the vortices are interacting directly with the dots for $B<B_1$, but reside in interstitial potential wells for $B>B_1$ [see Fig. 5(a) for $n=1$ and 2]. Consequently, the resistivity should show a substantial increase immediately above the first-order matching field,[26] contrary to the experimental data.

In contrast, the multivortex model should basically show a field-independent pinning, since the vortices are confined to the magnetic dots[26] [see Fig. 5(b) for $n=1$ and 2]. This means that the strength of the fractional matching for $B>B_1$ is expected to be comparable to the one for $B<B_1$. In reality it is slightly weaker, due to the additional repulsive interaction with the other flux quantum which is allocated to the dot. This picture is in agreement with the experimental data for $B<B_{\mathrm{tr}}$.

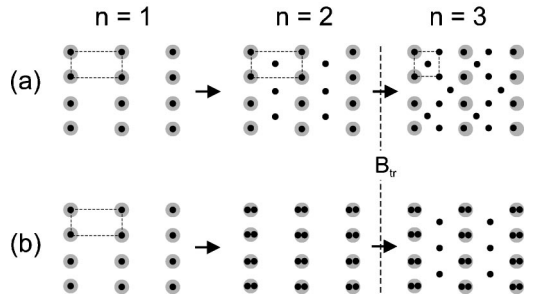

FIG. 5. Comparison of (a) the ''matched lattice'' model and (b) the ''multivortex'' model. The sketch shows the situation schematically for matching fields of orders $n=1$ and 2 before reconfiguration and for order $n=3$ after reconfiguration. The transition is symbolized by a dashed line. This situation resembles the one found in our experiments.

B. Transition region and high-field phase

The transition between the two regimes, which up to now we have called a ''reconfiguration transition,'' has a different explanation in the two models. For the multivortex model a change in behavior can be expected when the saturation number $n_s \approx 2$ for the dots is reached.[27,25] Above this saturation field, additional vortices have to sit at interstitial positions, as illustrated in Fig. 5(b) ($n=3$). Therefore, in this scenario, the transition is an indication of the formation of interstitial vortices. Such a coexistence between multiquanta and interstitial vortices was seen in Bitter decoration experiments with arrays of holes.[27] The absence of a fractional matching effect above B_{tr}, which was described in Sec. III A, could be another indication of a much weaker pinning due to these interstitial vortices. It was shown in theoretical simulations that these interstitials tend to move in channels, and produce no or much weaker fractional matching peaks.[26,28] However, as already discussed for the matched lattice model, the critical current of the interstitial vortices should be lower than that of the ones pinned at the dots, and consequently a substantial increase of resistivity should be observed immediately above the change of regime. In contrast, our data in Figs. 1 and 4 show that the absolute resistance value stays about the same or even decreases after the value B_{tr} is exceeded.

The presence of hysteresis in the change of regime implies the existence of an energy barrier between the two configurations, and thus may involve a first-order transition. For the multivortex model it was pointed out[27] that the transition between multiple vortices and interstitial vortices is indeed a first-order phase transition, which could explain the hysteretic magnetoresistance.

In the matched-lattice model, it was proposed[29] that a change of regime occurs as soon as the elastic energy of the vortex lattice E_{el} dominates over the pinning energy E_{pin}. Then the vortex lattice reconfigures from a commensurate

rectangular to a square configuration, as shown in Fig. 5(a) ($n=3$). This suggestion is based on the experimental fact that the series of maxima observed at high fields show a periodicity which seems to be related to the side of the rectangle along which the force is applied.[29] In this picture, the minima signal the matching of the vortex lattice parameter to the dot lattice parameter along the movement direction $a=na_0$, leading to a *dynamical* pinning. However, given that the vortex lattice parameter scales as $B^{-1/2}$, and $a_0=\sqrt{\phi_0/B}$, this line of reasoning would give rise to a *quadratic* rather than an *equally spaced* series of peaks: $B_n=n^2(\phi_0/a^2)$. This prediction is obviously very different from the *linearly equally spaced* series of peaks found experimentally.[29] This argument leads to the conclusion that an explanation of these features cannot be achieved with a simple lattice-matching argument. If this idea is to be developed further, other mechanisms have to be considered, such as a reorientation of the vortex lattice for different fields or a loss of coherence due to a mismatch along the applied current direction with a simultaneous matching along the force direction.

The hysteresis cannot be easily understood in the matched-lattice model. To pin and depin the lattice, the vorticity at the dots has to change between 1 and 0, but this change does not present an energy barrier for a hole in a superconductor.[30] If the observed change of regime is indeed an indication of a change of the lattice geometry, then a barrier should exist between these two configurations.

Up to this point we have discussed our results in terms of *static* models, implicitly thinking of a vortex lattice being geometrically commensurate or incommensurate with a fixed dot array. However, it was already mentioned that there is clear-cut evidence pointing to the presence of *dynamical* effects in the magnetoresistance. For example, it was recently shown that the observed features in the magnetoresistance are strongly dependent on the vortex velocity.[31] Also, it was found that the position of the minima for samples with rectangular arrays of magnetic dots depends on the direction of the applied current.[21] The importance of a dynamical ordering of the vortex lattice under the influence of periodic pinning was recently stressed in studies of the vortex lattice structure using Bitter pinning.[9] It was found that if a vortex lattice is driven by a change in the direction of the applied field, the very weak periodic pinning caused by a pattern of Fe clumps produced in a first Bitter decoration experiment can dominate over the bulk pinning in spite of being orders of magnitude smaller.

Recent simulations of driven vortex movement in the presence of rectangular arrays of pinning centers[32,28] clearly show the formation of channels between the rows of dots. These results offer an interesting and intriguing possibility for the analysis of our experimental results. In this scenario, channels of moving vortices between two consecutive rows of dots would dynamically order to form a lattice, infinite in the direction of movement but finite in the perpendicular direction. In this situation, the vortices pinned to the dots form a repulsive periodic potential. Thus the edges of the moving lattice experience a periodic perturbation, the time scale of which depends only on the lattice parameter of the array along the movement direction. This corresponds to a frequency $f=a/v$, where v is the lattice velocity. A similar effect was seen for a periodic pinning in superlattices in which the vortices move perpendicularly to the layers.[33] However, at this moment it is not clear to us how this perturbation and its interaction with the dynamical states of the moving lattice would translate to the structure observed for the high-field phase.

V. SUMMARY AND CONCLUSIONS

We have investigated periodic vortex pinning in rectangular arrays of magnetic dots. In our magnetoresistance measurements we found a strong fractional matching effect up to the second-order matching field. For magnetic fields larger than a threshold value B_{tr}, a distinct change in behavior occurs in this type of pinning array. Above this field, the fractional matching is absent or at least much weaker than below B_{tr}.

We also observed an interesting hysteretic effect in the magnetoresistance curves when the magnetic field is swept above the reconfiguration threshold and back again. We showed that this effect does not appear if this threshold B_{tr} is not exceeded. Additionally, we also find the same effect in samples with nonmagnetic pinning centers. Therefore, we conclude that it is correlated to the ''transition'' B_{tr} rather than to the magnetic moments of the dots.

Our experimental data suggest that a model including multivortex pinning explains our data better than a model based on the formation of interstitials. We argue that the observed transition could be due to a crossover from multivortex to interstitial vortex pinning. This explanation would explain the observed hysteretic behavior in terms of a first-order transition. It is likely that dynamical effects, such as the dynamic ordering of the lattice and the formation of channels, also have to be taken into account in order to explain the high-field behavior of the magnetoresistance. In order to resolve these issues, experiments which directly image the vortex configuration and correlations with the transport measurements could be useful.

ACKNOWLEDGMENTS

This work was supported by DOE and NSF. O.M.S. acknowledges support from the Deutscher Akademischer Austauschdienst (DAAD). J.G. acknowledges support from the Fulbright Commission and Fundación Antorchas during his visit to UCSD. J.G. is also a CONICET (Argentina) fellow. M.I.M. thanks the Spanish Secretaría de Estado de Universidades e Investigación for supporting her stay at UCSD.

*Present address: Motorola Labs, 7700 South River Parkway ML34, Tempe, Arizona 85284.

[1] G. Blatter, M. V. Feigel'man, V. B. Geshkenbein, A. I. Larkin, and V. M. Vinokur, Rev. Mod. Phys. **66**, 1125 (1994).
[2] G. W. Crabtree and D. R. Nelson, Phys. Today **50** (4), 38 (1997).
[3] A. T. Fiory, A. F. Hebard, and S. Somekh, Appl. Phys. Lett. **32**, 73 (1978).
[4] M. Baert, V. V. Metlushko, R. Jonckhere, V. V. Moshchalkov, and Y. Bruynserade, Phys. Rev. Lett. **74**, 3269 (1995).
[5] V. V. Metlushko, M. Baert, R. Jonckhere, V. V. Moshchalkov, and Y. Bruynserade, Solid State Commun. **91**, 331 (1994).
[6] V. V. Metlushko, U. Welp, G. W. Crabtree, R. Osgood, S. D. Bader, L. E. DeLong, Z. Zhang, S. R. J. Brueck, B. Ilic, K. Chung, and P. J. Hesketh, Phys. Rev. B **60**, 12 585 (1999).
[7] J. I. Martín, M. Vélez, J. Nogúes, and I. K. Schuller, Phys. Rev. Lett. **79**, 1929 (1997).
[8] Y. Jaccard, M.-C. Cyrille, M. Velez, J. L. Vicent, and I. K. Schuller, Phys. Rev. B **58**, 8232 (1998).
[9] Y. Fasano, M. Menghini, F. de la Cruz, and G. Nieva, Phys. Rev. B **62**, 15183 (2000).
[10] P. Selders, A. M. Castellanos, M. Vaupel, and R. Wördenweber, IEEE Trans. Appl. Supercond. **9**, 2967 (1999).
[11] M. I. Montero, J. J. Åkerman, A. Varilci, and I. K. Schuller (unpublished).
[12] M. J. Van Bael, L. Van Look, K. Temst, M. Lange, J. Bekaert, U. May, G. Güntherodt, V. V. Moshchalkov, and Y. Bruynseraede, Physica C **332**, 12 (2000).
[13] A. Hoffmann, P. Prieto, and I. K. Schuller, Phys. Rev. B **61**, 6958 (2000).
[14] D. J. Morgan and J. B. Ketterson, Phys. Rev. Lett. **80**, 3614 (1998).
[15] J. I. Martín, M. Vélez, A. Hoffmann, I. K. Schuller, and J. L. Vicent, Phys. Rev. Lett. **83**, 1022 (1999).
[16] A. E. Koshelev and V. M. Vinokur, Phys. Rev. Lett. **73**, 3580 (1994).
[17] U. Yaron, P. L. Gammel, D. A. Huse, R. N. Kleiman, C. S. Oglesby, B. Bucher, B. Batlogg, D. J. Bishop, K. Mortensen, K. Clausen, C. A. Bolle, and F. De La Cruz, Phys. Rev. Lett. **73**, 2748 (1994).
[18] A. Duarte, F. E. Righi, C. A. Bolle, F. de la Cruz, P. L. Gammel, C. S. Oglesby, B. Bucher, B. Batlogg, and D. J. Bishop, Phys. Rev. B **53**, 11 336 (1996).
[19] F. Pardo, F. De La Cruz, P. L. Gammel, C. S. Oglesby, E. Bucher, B. Batlogg, and D. J. Bishop, Phys. Rev. Lett. **78**, 4633 (1997).
[20] G. Carneiro, Phys. Rev. B **62**, R14 661 (2000).
[21] J. I. Martín, Y. Jaccard, A. Hoffmann, J. Nogués, J. M. George, J. L. Vicent, and I. K. Schuller, J. Appl. Phys. **84**, 411 (1998).
[22] M. I. Montero, J. J. Åkerman, and I. K. Schuller (unpublished).
[23] E. Rosseel, M. J. Van Bael, M. Baert, R. Jonckheere, V. V. Moshchalkov, and Y. Bruynserade, Phys. Rev. B **53**, 2983 (1996).
[24] J. Wittborn, K. V. Rao, J. Nogués, and I. K. Schuller, Appl. Phys. Lett. **76**, 2931 (2000).
[25] G. S. Mkrtchyan and V. V. Shmidt, Zh. Eksp. Teor. Fiz. **61**, 367 (1971) [Sov. Phys. JETP **34**, 195 (1972)].
[26] C. Reichhardt, G. T. Zimanyi, R. T. Scalettar, A. Hoffmann, and I. K. Schuller, Phys. Rev. B **64**, 052503 (2001).
[27] A. Bezryadin and B. Pannetier, J. Low Temp. Phys. **102**, 102 (1996).
[28] C. Reichhardt, G. T. Zimanyi, and N. Grønbech-Jensen, Phys. Rev. B **64**, 014501 (2001).
[29] J. I. Martín, M. Vélez, A. Hoffmann, I. K. Schuller, and J. L. Vicent, Phys. Rev. B **62**, 9110 (2000).
[30] A. Bezryadin, A. Buzdin, and B. Pannetier, Phys. Rev. B **51**, 3718 (1995).
[31] M. Veléz, D. Jaques, J. I. Martín, F. Guinea, and J. L. Vicent, cond-mat/0104152 (unpublished).
[32] C. Reichhardt, R. T. Scalettar, G. T. Zimanyi, and N. Grønbech-Jensen, Phys. Rev. B **61**, R11 914 (2000).
[33] A. Gurevich, E. Kadyrov, and D. C. Larbalestier, Phys. Rev. Lett. **77**, 4078 (1996).